

A Comparison of Stellar Kinematics Derived from Two Gemini NIFS Reduction Pipelines

Katie A. Merrell¹, Misty C. Bentz¹ , and Jonelle L. Walsh² 

Published December 2020 • © 2020. The American Astronomical Society. All rights reserved.

Research Notes of the AAS, Volume 4, Number 12

Citation Katie A. Merrell *et al* 2020 *Res. Notes AAS* **4** 250

¹ Georgia State University, USA

² Texas A&M University, USA

Misty C. Bentz  <https://orcid.org/0000-0002-2816-5398>

Jonelle L. Walsh  <https://orcid.org/0000-0002-1881-5908>

Received December 2020

Accepted December 2020

Published December 2020

<https://doi.org/10.3847/2515-5172/abd637>

Stellar kinematics; Astronomy data reduction; AGN host galaxies

 Journal RSS

Sign up for new issue notifications

Create citation alert

Abstract

The Gemini Near-infrared Integral Field Spectrograph (NIFS) reduction pipeline is widely used to reduce NIFS data. However, there are critical known limitations. A new NIFS reduction pipeline has recently been developed and solves several of these problems. We present a comparison of stellar kinematics derived from the new and old data reduction pipelines, as well as recommendations for optimal NIFS data reduction.

This site uses cookies. By continuing to use this site you agree to our use of cookies. To find out more, see our [Privacy and Cookies policy](#).



Export citation and abstract

BibTeX

RIS

[◀ Previous article in issue](#)[Next article in issue ▶](#)

1. Introduction

The ability to simultaneously obtain spectra over a two-dimensional field of view using integral field spectroscopy revolutionized studies of extended objects (Cappellari 2016). While long-slit spectrographs collect spectra along a narrow slice, Integral Field Spectrographs (IFSs) partition the full two-dimensional field of view and produce spectra at each spatial position with one exposure. In this way, IFSs are more time efficient for studying the motions of gas and stars in extended objects than long-slit spectroscopy, which requires multiple exposures to acquire spectra across the whole field.

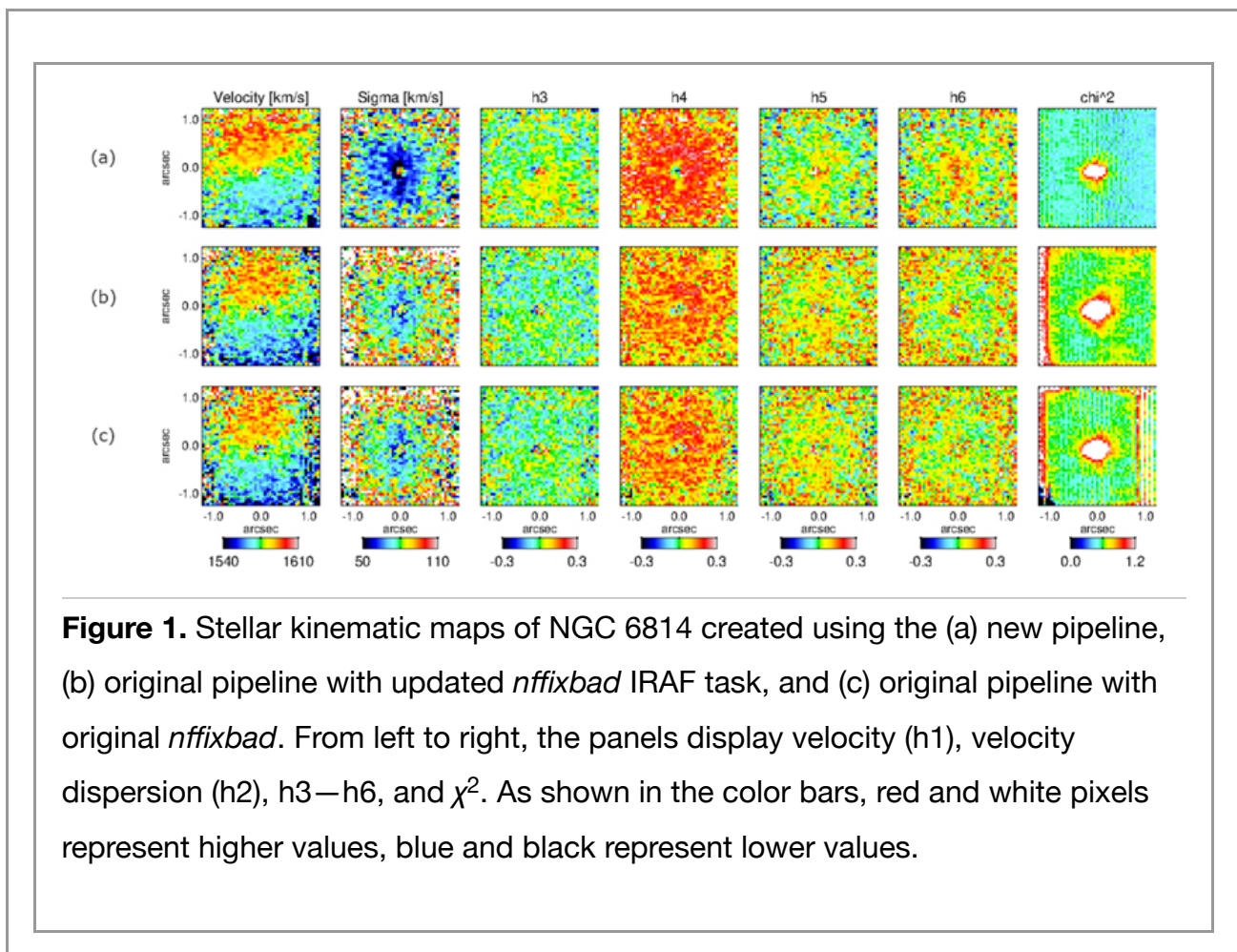
In the near-infrared, IFSs paired with adaptive optics are optimally suited for studying stellar and gas kinematics in very compact regions. When used with adaptive optics, the Near-infrared Integral Field Spectrograph (NIFS) on Gemini North can isolate regions of about 01 on the sky, similar to the near-infrared spatial resolution provided by the Hubble Space Telescope. NIFS divides the 3'' × 3'' field of view into 29 vertical slices (McGregor et al. 2003) and each slice is dispersed and stacked vertically on the detector. The reduction pipeline converts two-dimensional raw science frames into reduced three-dimensional data cubes consisting of two spatial dimensions and one spectral dimension. IRAF scripts are provided on the Gemini NIFS website,³ but they do not implement flux calibration, variance propagation, heliocentric velocity corrections, or a recipe for combining science exposures. A new reduction pipeline⁴ was constructed to mitigate these limitations and improve the original pipeline. To properly compare the results from both pipelines, we developed scripts to add some of the missing capabilities to the existing pipeline. We reduced raw NIFS observations of the nucleus of Seyfert galaxy NGC 6814 (GN-2013B-Q-5, PI: Misty Bentz) using both pipelines and we present a comparison of the methods and resultant stellar kinematics.

This site uses cookies. By continuing to use this site you agree to our use of cookies. To find out more, see our [Privacy and Cookies policy](#).



2. Analysis

Both pipelines begin with baseline calibrations, carrying out the same routines for flat-fielding, dark subtraction, sky subtraction, determining the wavelength solutions, and generating the spatial calibration files. A notable distinction is the improvement made to bad pixel masking in the new pipeline. The IRAF task *nffixbad* creates a mask for each science frame to eliminate bad pixels (due to cosmic rays, etc.). When *nffixbad* locates a bad pixel in a science extension, it interpolates across the pixel and replaces the value, but in the variance extension, *nffixbad* sets the matching pixel to a high value, creating a noise spike. In the stellar kinematic maps displayed in Figure 1(c), the excess noise from the original version of *nffixbad* can be seen as striping patterns near the edges of the maps. The new pipeline incorporates a modified version of *nffixbad* that treats the variance in the same way as the science.



After the baseline calibration files are processed, the telluric corrections are produced. In both reduction tasks, *PyRAF* extracts the slit spectra from each detector frame within

a default aperture radius, then combines them into a single spectrum for each star per night. The stellar continuum and absorption lines are then removed, leaving only the telluric features. In the original pipeline, this is achieved by fitting each nightly telluric spectrum with a blackbody curve and interpolating over the strong stellar absorption lines by hand with the IRAF task *splot*. To more accurately remove the stellar components, we modified the original pipeline to incorporate Xtellcor (Vacca et al. 2003), which uses a model Vega (A0V) spectrum to simulate the observed star spectrum. The new pipeline telluric spectra are instead fitted with multiple A-star Kurucz models to simulate and remove the stellar features. Additionally, the new pipeline converts one of the star frames on a given night into a data cube, which is later used to flux calibrate the galaxy frames.

The original pipeline only propagates the variances up to the telluric corrections. It is left to the user to develop a method that propagates the variances through to the final data cubes. We constructed our own script for this purpose, so as to properly compare the two pipelines. A meaningful improvement in the new pipeline is that it efficiently carries the variances through the end of the reductions.

After the telluric corrections are applied, the galaxy frames are transformed into data cubes. In the original pipeline, the slices in each galaxy frame are rectified into an individual data cube per frame. Spatial offsets between the individual cubes are determined by the user in increments of whole pixels, then the IRAF task *imcombine* shifts and combines the individual cubes while providing an optional pixel value rejection scheme. The new pipeline rectifies, aligns, and combines the galaxy frames into a final data cube in a single step. In addition, fractional pixel offsets allow the spatial resolution to be preserved. However, no pixel value rejection scheme is employed, so some additional noise may be retained.

Finally, observations obtained over the course of several months require correction for the motion of the Earth around the Sun. The original pipeline does not provide a correction to heliocentric velocities. We developed a script to determine the heliocentric velocity correction for nightly combined cubes using the IRAF task *rvcorrect*, apply the corrections in velocity space, then combine the cubes as a weighted mean. The new pipeline applies a heliocentric velocity correction to each galaxy frame as it is rectified and combined.

This site uses cookies. By continuing to use this site you agree to our use of cookies. To find

out more, see our [Privacy and Cookies policy](#).

Although not included in this comparative analysis, the new pipeline produces a single



merged sky cube from the reduced sky exposures and measures the line spread-function as a function of spatial location by fitting Gaussians to sky lines.

Observations of NGC 6814 were reduced with the new pipeline and the original pipeline with modifications described above. Stellar kinematic maps were then created using the Penalized-Pixel Fitting method (pPXF; Cappellari & Emsellem 2004; Cappellari 2017), which uses stellar absorption features in galaxy spectra to characterize the bulk motions of stars. The stellar kinematics are constrained by convolving stellar template spectra with a line-of-sight velocity distribution (LOSVD) to match the observed galaxy spectra. pPXF parameterizes the shape of the LOSVD using Gauss-Hermite polynomials. Figure 1 shows the stellar kinematic maps derived from the new pipeline (Figure 1(a)) and two modified versions of the original pipeline, with the only difference being that one incorporates the improved version of the *nfixbad* task (Figure 1(b)), and the other retains the original version (Figure 1(c)). The panels display velocity (h1), velocity dispersion (h2), higher order Gauss-Hermite terms h3–h6, and χ^2 .

Although the kinematic maps are similar, the new pipeline yields lower velocity dispersions, higher h4 values, and smoother maps that include similar χ^2 values across the field with a more compact region of central high values associated with the active galactic nucleus (AGN). Taking advantage of the unresolved AGN, we fit the resultant point-spread function (PSF) of each data cube with two nested Gaussians. The new pipeline produces a more circular and compact PSF, demonstrating an improved ability to maintain spatial resolution. Thus, we recommend the new pipeline for NIFS reductions, but note that a method for dealing with the additional noise, such as the CLEAN parameter in pPXF, should be applied. And for those who choose to use the original pipeline, we recommend replacing the default *nfixbad* task with the improved version.

M.C.B. and K.M. are supported by the NSF through grant AST-2009230 to Georgia State University.

Footnotes

³ www.gemini.edu/instrumentation/nifs/data-reduction

⁴ Developed by Jonelle Walsh, Anil Sethi, Richard McDermid, Nora Luetzgendorf, and this site was developed by continuing to use this site. You agree to our use of cookies to enhance your navigation. Our cookie policy can be found at www.gemini.edu/instrumentation/nifs/data-reduction and our privacy policy at www.gemini.edu/instrumentation/nifs/data-reduction.
 out more by <https://github.com/jlwalsh12/NIFS-reduction-pipeline>.

[↑](#) Cappellari M. 2016 *ARA&A* **54** 597

[Crossref](#) [ADS](#) [Google Scholar](#)



[↑](#) Cappellari M. 2017 *MNRAS* **466** 798

[Crossref](#) [ADS](#) [Google Scholar](#)



[↑](#) Cappellari M. and Emsellem E. 2004 *PASP* **116** 138

[IOPscience \(https://iopscience.iop.org/1538-3873/116/816/138\)](https://iopscience.iop.org/1538-3873/116/816/138) [ADS](#) [Google Scholar](#)



[↑](#) McGregor P. J., Hart J., Conroy P. G. *et al* 2003 *Proc. SPIE* **4841** 1581

[Crossref](#) [ADS](#) [Google Scholar](#)



[↑](#) Vacca W. D., Cushing M. C. and Rayner J. T. 2003 *PASP* **115** 389

[IOPscience \(https://iopscience.iop.org/1538-3873/115/805/389\)](https://iopscience.iop.org/1538-3873/115/805/389) [ADS](#) [Google Scholar](#)



Export references:

[BibTeX](#)

[RIS](#)

